Yeast two-hybrid screening

We performed yeast two-hybrid experiments with a *Hydra vulgaris* two-hybrid cDNA library (Stratagene) as described by the supplier. The *Hyβ-Cat* bait (amino acids 166–586) was cloned to the GAL4 DNA-binding domain in the pBD phagemid vector. The bait was transformed into the yeast strain YRG-2 together with the cDNA library fused to the GAL4 activation domain in the pAD phagemid vector. Interacting proteins were selected on plates lacking histidine and containing 3-aminotriazole (10 mM). We tested activation of a second reporter gene, lacZ, by filter lift assay.

Xenopus embryo injection

Xenopus embryos were generated by *in vitro* fertilization, dejellied and further cultivated. Dorsal–ventral polarity was determined at the four-cell stage, and darker, ventral blastomers were injected with 4 nl synthetic mRNA (2–4 ng). For mRNA synthesis, linearized pBS-plasmid containing full-length *Hyβ-Cat* cDNA was transcribed using a T3 Message Machine Kit (Ambion).

In situ hybridization

Whole mount *in situ* hybridization with DIG-labelled RNA probes was done as described[30].

RT–PCR

A cDNA template was produced using Ready-To-Go First-Strand Beads (Pharmacia) from total RNA isolated from the distal fifth of head regenerates. We detected *Hyβ-Cat* using the following primers: β-Cat forward (5′-CATTCTCGAAATGATGGC-3′) and β-Cat reverse (5′-CGCGTGGTAAAAACACA-3′). A 75-base pair (bp) intron located between these two primer sites in the *Hyβ-Cat* gene served as a control for genomic contamination. *Hydra EF1α* (GenBank accession number: Z68181) was detected using the primers EF1 forward (5′-GTTTGAAGCTGGTATTTC-3′) and EF1 reverse (5′-TGTTTACCAGTATCTTTG-3′). PCR conditions: 5 min 95 °C (1 cycle); 1 min 95 °C, 1 min 46 °C, 1 min 72 °C (35 cycles); 5 min 72 °C (1 cycle). Amplification products were quantified by optical density analysis (Image Master VDS, Pharmacia).

Hydra tissue manipulations

Hydra mass culture was maintained in a daily feeding regime[30]. All experimental animals were starved for 24 h. For head regeneration, polyps were bisected at 75% body length (one-quarter below the hypostome) and the proximal pieces were immediately transferred into fresh culture medium for further head regeneration. For dissociation and reaggregation, heads and feet were removed from 300 animals. The remaining body columns were then mechanically dissociated in hypotonic dissociation medium and reaggregated[12].

Received 24 February; accepted 20 July 2000.

1. Cadigan, K. M. & Nusse, R. Wnt signalling: a common theme in animal development. *Genes Dev.* **11**, 3286–3305 (1997).
2. Cox, R. T. & Peifer, M. Wingless signalling: The inconvenient complexities of life. *Curr. Biol.* **8**, R140–R144 (1998).
3. Hobmayer, E. *et al.* Identification of a hydra homologue of the β-catenin/plakoglobin/armadillo gene family. *Gene* **172**, 155–159 (1996).
4. Minobe, S. *et al.* Identification and characterization of the epithelial polarity receptor "Frizzled" in *Hydra vulgaris*. *Dev. Genes Evol.* **210**, 258–262 (2000).
5. Molenaar, M. *et al.* XTcf-3 transcription factor mediates β-catenin-induced axis formation in *Xenopus* embryos. *Cell* **86**, 391–399 (1996).
6. Bode, P. M. & Bode, H. R. in *Pattern Formation. A Primer in Developmental Biology* (eds Malacinski, G. M. & Bryant, S. V.) 213–241 (Macmillan, New York, 1984).
7. Meinhardt, H. A model for pattern formation of hypostome, tentacles, and foot in hydra: How to form structures close to each other, how to form them at a distance. *Dev. Biol.* **157**, 321–333 (1993).
8. Wolpert, L. *Principles of Development* (Oxford Univ. Press, Oxford, 1998).
9. Niehrs, C. & Pollet, N. Synexpression groups in eukaryotes. *Nature* **402**, 483–487 (1999).
10. Otto, J. J. & Campbell, R. D. Budding in *Hydra attenuata*: Bud stages and fate map. *J. Exp. Zool.* **200**, 417–428 (1977).
11. Achermann, J. & Sugiyama, T. Genetic analysis of developmental mechanisms in Hydra. X. Morphogenetic potentials of a regeneration-deficient strain (reg-16). *Dev. Biol.* **107**, 13–27 (1985).
12. Gierer, A. *et al.* Regeneration of hydra from reaggregated cells. *Nature New Biol.* **239**, 98–101 (1972).
13. Gierer, A. & Meinhardt, H. A theory of biological pattern formation. *Kybernetik* **12**, 30–39 (1972).
14. MacWilliams, H. K. *Hydra* transplantation phenomena and the mechanism of *Hydra* head regeneration. II. Properties of head activation. *Dev. Biol.* **96**, 239–257 (1983).
15. van de Wetering, M. *et al.* Armadillo coactivates transcription driven by the product of the *Drosophila* segment polarity gene *dTCF*. *Cell* **88**, 789–799 (1997).
16. Lessing, D. & Nusse, R. Expression of wingless in the *Drosophila* embryo: a conserved *cis*-acting element lacking conserved Ci-binding sites is required for patched-mediated repression. *Development* **125**, 1469–1476 (1998).
17. Conway Morris, S. Metazoan phylogenies: falling into place or falling to pieces? A palaeotological perspective. *Curr. Op. Genet. Dev.* **8**, 662–667 (1998).
18. Aguinaldo, A. M. A. *et al.* Evidence for a clade of nematodes, arthropods and other moulting animals. *Nature* **387**, 489–493 (1997).
19. Knoll, A. H. & Carroll, S. B. Early animal evolution: Emerging views from comparative biology and geology. *Science* **284**, 2129–2137 (1999).
20. Slack, J. M. W., Holland, P. W. H. & Graham, C. F. The zootype and the phylotypic stage. *Nature* **361**, 490–492 (1993).
21. Finnerty, J. R. & Martindale, M. Q. The evolution of the Hox cluster: insights from outgroups. *Curr. Op. Genet. Dev.* **8**, 681–687 (1998).
22. Kuhn, K., Streit, B. & Schierwater, B. Isolation of Hox genes from the scyphozoan *Cassiopeia xamachana*: Implications for the early evolution of Hox genes. *Mol. Dev. Evol.* **285**, 63–75 (1999).
23. Gauchat, D. *et al.* Evolution of Antp-class genes and differential expression of Hydra Hox/paraHox genes in anterior patterning. *Proc. Natl Acad. Sci. USA* **97**, 4493–4498 (2000).
24. Neumann, C. J. & Cohen, S. M. Long-range action of Wingless organizes the dorsal-ventral axis of the *Drosophila* wing. *Development* **124**, 871–880 (1997).
25. Kopp, A., Blackman, R. K. & Duncan, I. Wingless, Decapentaplegic and EGF receptor signalling pathways interact to specify dorso-ventral pattern in the adult abdomen of *Drosophila*. *Development* **126**, 3495–3507 (1999).
26. Larabell, C. A. *et al.* Establishment of the dorso-ventral axis in *Xenopus* embryos is presaged by early asymmetries in β-catenin that are modulated by the Wnt signalling pathway. *J. Cell Biol.* **136**, 1123–1136 (1997).
27. Willmer, P. *Invertebrate Relationships. Patterns in Animal Evolution* (Cambridge Univ. Press, Cambridge, UK, 1990).
28. Nielsen, C. *Animal Evolution: Interrelationships of the Living Phyla* (Oxford Univ. Press, Oxford, 1995).
29. Frohman, M. A. in *PCR Primer—A Laboratory Manual* (eds Dieffenbach, C. W. & Dveksler, G. S.) 381–409 (CSHL, New York, 1995).
30. Technau, U. & Bode, H. R. *HyBra1*, a brachyury homologue, acts during head formation in hydra. *Development* **126**, 999–1010 (1999).

Identification of a vesicular glutamate transporter that defines a glutamatergic phenotype in neurons

Shigeo Takamori*, Jeong Seop Rhee†, Christian Rosenmund† & Reinhard Jahn*

* *Department of Neurobiology and* † *Department of Membrane Biophysics, Max-Planck-Institute for Biophysical Chemistry, Am Faβberg 11, D-37077 Göttingen, Germany*

Glutamate is the major excitatory neurotransmitter in the mammalian central nervous system. Synaptic vesicles are loaded with neurotransmitter by means of specific vesicular transporters. Here we show that expression of BNPI, a vesicle-bound transporter associated with sodium-dependent phosphate transport[1–3], results in glutamate uptake by intracellular vesicles. Substrate specificity and energy dependence are very similar to glutamate uptake by synaptic vesicles. Stimulation of exocytosis—fusion of the vesicles with the cell membrane and release of their contents—resulted in quantal release of glutamate from BNPI-expressing cells. Furthermore, we expressed BNPI in neurons containing GABA (γ-aminobutyric acid) and maintained them as cultures of single, isolated neurons that form synapses to themselves. After stimulation of these neurons, a component of the postsynaptic current is mediated by glutamate as it is blocked by a combination of the glutamate receptor antagonists, but is insensitive to a GABA_A receptor antagonist. We conclude that BNPI functions as vesicular glutamate transporter and that expression of BNPI suffices to define a glutamatergic phenotype in neurons.

Specific vesicular transporters are responsible for loading synaptic vesicles with neurotransmitters. Unlike transporters at the plasma membrane, these are driven by an electrochemical proton gradient across the vesicle membrane. Proteins responsible for

transporting acetylcholine, monoamines and GABA have been identified at the molecular level[4]. However, the protein responsible for glutamate uptake into synaptic vesicles has eluded detection. In our search for the vesicular glutamate transporter, proteins of highly purified synaptic vesicles from rat brain were separated by two-dimensional electrophoresis[5]. Internal sequences were then obtained from a spot with an apparent relative molecular mass of about 65,000 ($M_r \approx 65K$) that was separated from the co-migrating synaptotagmin (not shown). In addition to peptide sequences corresponding to synaptotagmin, tubulin and the vesicular GABA transporter (VGAT), three sequences were obtained (GGHVVVQK, WAPPLER, FNTPWR) which correspond to BNPI, the brain-specific Na^{+}-dependent inorganic phosphate co-transporter I (ref. 1).

BNPI encodes a membrane protein with 6–8 putative transmembrane domains which exhibits weak similarities to a kidney Na^{+}-dependent inorganic phosphate co-transporter. When BNPI was expressed in *Xenopus* oocytes, Na^{+}-dependent uptake of inorganic phosphate was observed[1]. Surprisingly, however, the transporter is predominantly localized to synaptic vesicles of excitatory-type asymmetric synapses[3]. Furthermore, loss-of-function mutations in eat-4, a BNPI homologue in *C. elegans*, caused severe deficiencies of glutamate-mediated neurotransmission whereas other neuronal functions were not affected. Iontophoretic application of glutamate showed normal responses, indicating that the impairment was caused by a presynaptic defect[6]. We therefore investigated whether BNPI may function as a vesicular glutamate transporter in glutamate-releasing terminals.

First, we examined whether BNPI is specifically localized to synaptic vesicles containing glutamate in the brain. Using a peptide corresponding to BNPI residues 24–38 as antigen, a rabbit antiserum was generated that was further affinity-purified on immobilized peptide. The antibody recognized a major band of $M_r \approx 60K$ that co-purified with synaptic vesicles upon subcellular fractionation (Fig. 1a). We then immobilized the antibodies on methacrylate microbeads[7] to immuno-isolate BNPI-containing vesicles. As shown in Fig. 1b, BNPI immuno-isolates are devoid of both VGAT and the vesicular monoamine transporter 2 (VMAT2), whereas other synaptic vesicle proteins are present including the M_r 116K subunit of the vacuolar proton pump, the enzyme that drives neurotransmitter uptake. In contrast, VGAT immuno-isolates were devoid of BNPI and VMAT2. Immuno-isolated fractions were then assayed for proton-gradient-dependent uptake of glutamate and GABA. BNPI immuno-isolates showed high glutamate-uptake activity and low GABA-uptake activity, whereas VGAT immuno-isolates showed exactly the opposite pattern (Fig. 1c, see also ref. 7). Together these results confirm that BNPI is selectively localized on vesicles containing glutamate.

To examine whether BNPI may function as a vesicular glutamate transporter, the transporter was expressed in BON cells, a neuroendocrine serotonin-secreting cell line[8]. Two stable, BNPI-expressing cell lines were generated (BNPI-5, BNPI-36) in which BNPI is predominantly localized to intracellular membranes (Fig. 2a). A membrane fraction was isolated from these cells and tested for glutamate uptake activity. Membranes of the BNPI-expressing cell lines exhibited ATP-dependent glutamate uptake that was sensitive to the uncoupler carbonyl cyanide *p*-(trifluoromethoxy)phenylhydrazone (FCCP) (Fig. 2b and c). As control, we used membranes prepared from cells transfected either with VGAT or with vector alone. Although some time-dependent glutamate accumulation was observed in those cell lines, this activity was not inhibited by FCCP. In contrast, membranes prepared from VGAT-expressing cells exhibited FCCP-sensitive GABA-uptake activity that was significantly higher than the background activity observed in vector-transfected or BNPI-expressing cells (Fig. 2c).

The vesicular glutamate transporter is known to prefer glutamate over aspartate, in contrast to the Na^{+}-dependent transport systems[9].

Uptake of [³H]glutamate by the membrane extract was competed for by the addition of 10 mM L-glutamate (Fig. 2d). D-glutamate was less potent, whereas L-aspartate, GABA and glycine had no effect. Next, we investigated the energy dependence of glutamate uptake. In synaptic vesicles, the glutamate transporter is driven mainly by
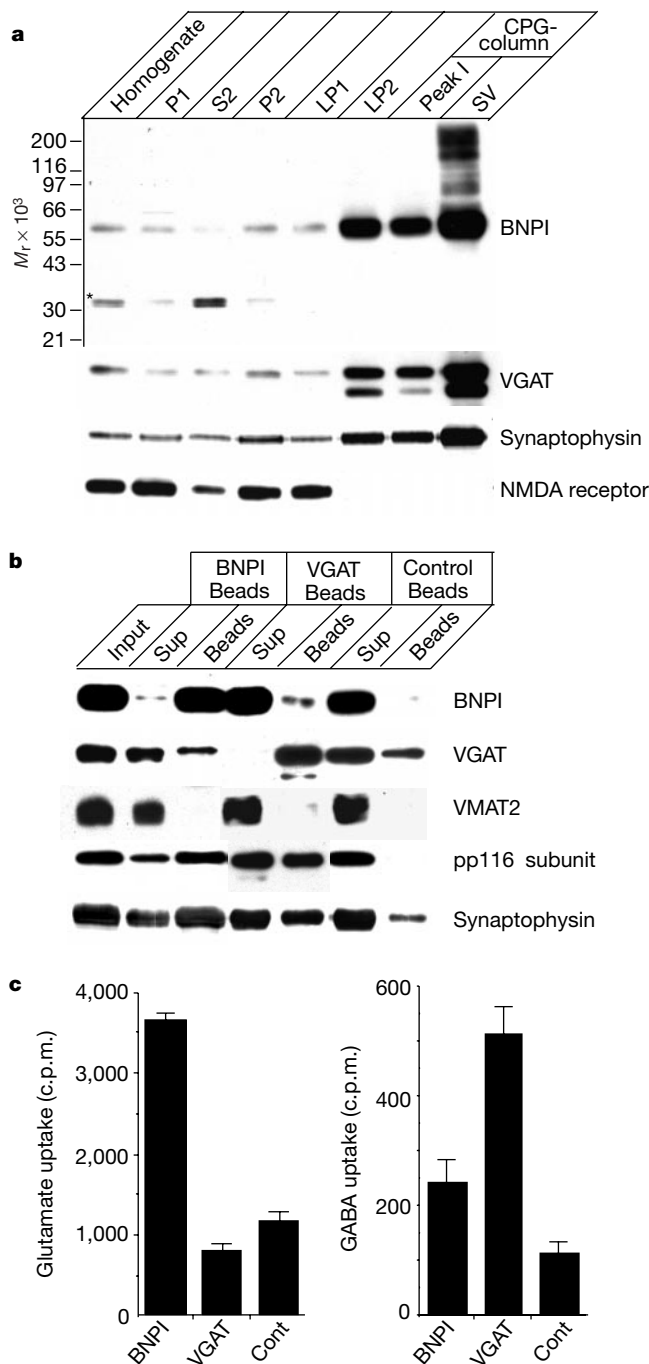

Figure 1 BNPI is exclusively present on glutamatergic synaptic vesicles. **a**, BNPI is enriched in synaptic vesicles. The fractions during synaptic vesicle purification were analysed for BNPI, VGAT, synaptophysin and NMDA receptor by immunoblotting. BNPI ($M_r \approx 60K$) is enriched in pure synaptic vesicle fraction (SV). Asterisk shows an additional immunoreactive band of lower M_r that is unrelated to BNPI and that is lost upon synaptic vesicle purification. **b**, Immuno-isolation of BNPI- and VGAT-containing vesicles shows that the transporters are present on separate populations of synaptic vesicles. Input (LP2), material not bound to the beads (Sup) and material bound to the beads (Beads) were analysed by immunoblotting. **c**, Vesicular glutamate and GABA uptake into bead-immunoisolates. The values represent FCCP-sensitive uptake.

the membrane-potential component of the proton electrochemical potential across the vesicle membrane, which is generated by a vacuolar proton ATPase[10]. Bafilomycin A$_1$ and N-ethylmaleimide (NEM) both specific inhibitors of vacuolar proton pumps, inhibited glutamate uptake, whereas inhibitors of mitochondrial F$_0$-F$_1$-ATPases and E$_1$-E$_2$-ATPases were ineffective (Fig. 2e). In addition, conditions known to reduce the membrane-potential component of the proton gradient (high chloride, electrogenic ionophore combinations) inhibited uptake, whereas a selective abolishment of the pH gradient (ammonium sulphate, nigericin) had only minor effects (Fig. 2f), in agreement with previous results on synaptic vesicles[11,12].

The results described above show that BNPI expression in BON cells leads to glutamate uptake in a vesicular compartment that is acidified by a vacuolar ATPase. BON cells contain secretory vesicles that can undergo regulated exocytosis in response to muscarinic stimulation[8]. We therefore asked whether BNPI expression would lead to accumulation of glutamate in secretory vesicles in addition to serotonin, and, consequently, whether glutamate is released upon stimulation in discrete quanta. To analyse for glutamate release, an excess of BNPI-expressing BON cells was co-cultured with HEK293 cells that were transiently transfected with a non-desensitizing

variant of the AMPA receptor[13]. To identify the BNPI- and glutamate-receptor (GluR)-expressing cells, green and red fluorescent proteins (EGFP and Ds-Red, respectively) were co-expressed using bi-cistronic constructs.

Whole-cell patch-clamp measurements were performed from GluR cells and their responsiveness to glutamate was tested by application of saturating concentration of L-glutamate (1 mM). Cells with robust responses (> 3 nA) were then placed in direct contact to BNPI cells. When exocytosis of the BNPI cells was stimulated by acetylcholine, transient miniature excitatory post-synaptic current (mEPSC)-like inward currents frequently developed in the GluR cells (14 out of 18 experiments; Fig. 3). These events were observed with an average frequency of 0.15 Hz. They produced inward currents with a peak amplitude of 51 ± 4 pA, a rise time of 4.1 ± 1.1 ms and a decay time constant of 24 ± 5 ms ($n = 275$, Fig. 3d). When the specific AMPA-receptor antagonist NBQX (30 μM, Fig. 3a) was added, the response was largely inhibited: spike-like events occurred with a 23-fold lower frequency (10 events in 1,200 s), and had an average amplitude of 22 ± 6 pA (false-positive events). No significant NBQX-sensitive activity could be recorded from VGAT-expressing cells regardless of whether NBQX was present or not ($n = 7$; Fig. 3d).
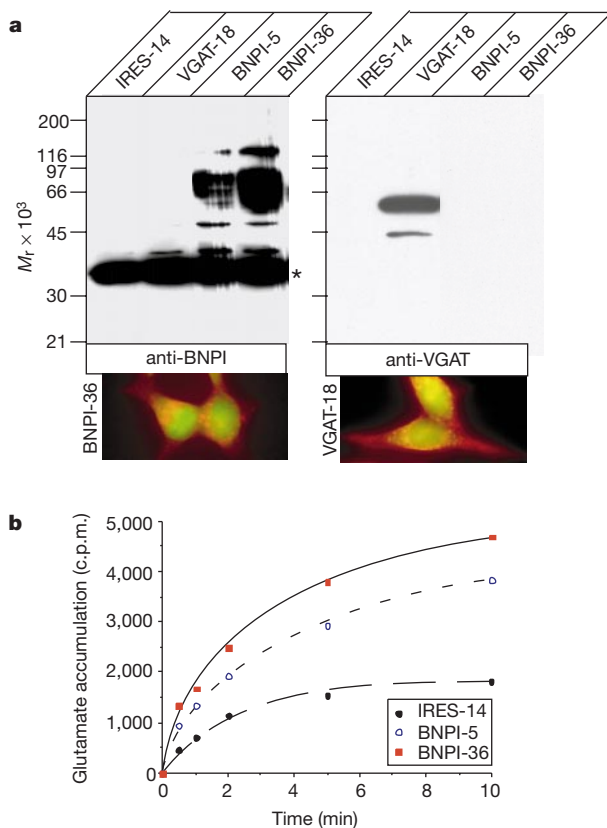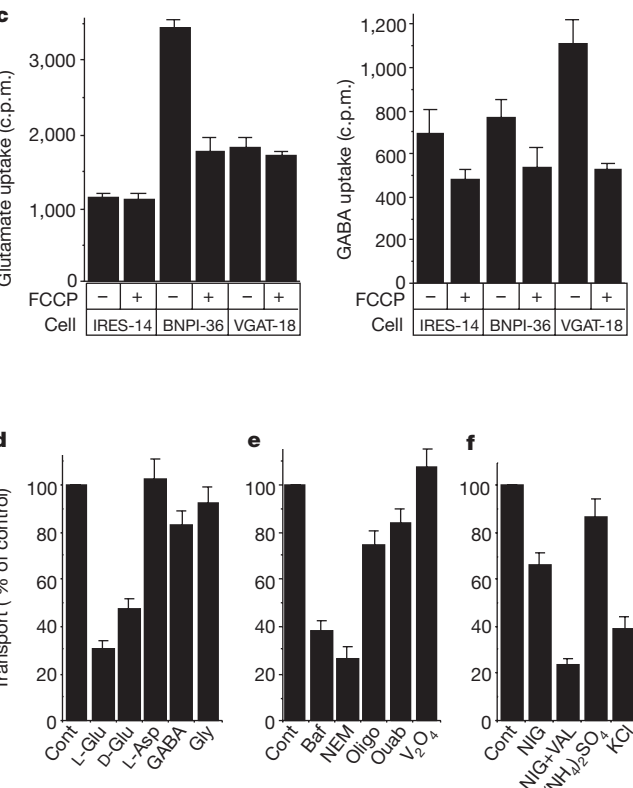

Figure 2 BNPI functions as a vesicular glutamate transporter. **a**, Intracellular expression of BNPI and VGAT in BON stable transfectants monitored by immunoblotting (top) and immunofluorescence (bottom, red). Asterisk, an unrelated immunoreactive band that is present in all cell clones (see also Fig. 1). Note that all stable transfectants express EGFP (bottom, green). **b**, Time dependence of [³H]L-glutamate accumulation of membranes isolated from BNPI-expressing clones (BNPI-5 and BNPI-36) compared with that from control clones (IRES-14). **c**, [³H]L-glutamate uptake by membranes from BNPI-expressing cells (BNPI-36) is sensitive to the uncoupler FCCP (left), whereas no such uptake is present in membranes from the other cell lines. By contrast, enhanced FCCP-sensitive [³H]GABA uptake is observed in VGAT-expressing clone (VGAT-18). **d**, Substrate specificity of glutamate uptake in BNPI-expressing cell membranes, measured by

competition of [³H]L-glutamate uptake with 10 mM unlabelled substrate. **e**, Glutamate uptake in BNPI-expressing cell membranes is driven by the vacuolar ATPase as it is inhibited by bafilomycin A$_1$ (Baf; 100 nM) and N-ethylmaleimide (NEM; 0.2 mM), but not by oligomycin B (Oligo; 5 μM), ouabain (Oub; 2 mM) or vanadate (V$_2$O$_4$; 50 μM). **f**, Glutamate uptake in BNPI-expressing cells depends more on the membrane potential than on the pH gradient, as shown by selective sensitivity towards specific inhibitors. The following concentrations were used: nigericin (NIG; 5 μM), valinomycin (VAL; 20 μM), (NH$_4$)$_2$SO$_4$ (10 mM), and KCl (100 mM). In **b**, **c**, background uptake was determined by incubation at 4 °C for 10 min. In **d–f**, values are expressed as percentage of control (without additives). Error bars, s.e.m. from at least two independent experiments using different membrane preparations.

Finally, we investigated whether expression of BNPI in neurons suffices to cause synaptic release of glutamate. For this purpose, autaptic hippocampal neurons were infected with a semliki-forest virus construct co-expressing BNPI and EGFP. EGFP-positive GABA-releasing neurons were selected for whole-cell recordings. In all cases we ensured that these cells were strictly isolated from other neurons. Autaptic responses were evoked by brief somatic depolarization (-70 mV to 0 mV for $1-2$ ms, Fig. 4). All cells exhibited a robust inhibitory postsynaptic current (IPSC, 4.3 ± 1.7 nA, $n = 9$). In uninfected cells, this current (4.2 ± 0.7 nA) was completely inhibited by the GABA$_A$-receptor antagonist bicuculline and picrotoxin ($n = 13$). In BNPI-expressing cells, however, we regularly (9 of 12 cells) observed a fast inward current component that was resistant to saturating concentrations of the bicuculline. This current component had an average amplitude of 208 ± 32 pA ($n = 9$) and was identified as a glutamate-mediated excitatory postsynaptic current (EPSC) as it was blocked by a combination of the AMPA-receptor and NMDA-receptor antagonists NBQX and AP5, respectively (Fig. 4d). The EPSC kinetics were slightly slower in rise and decay than expected from a normal glutamate-mediated EPSC (Fig. 4e, f). This is probably due to the fact that glutamate concentrations are lower in vesicles that contain both glutamate and GABA than in pure glutamate-containing vesicles, leading to lower receptor occupancy and activation kinetics. Alternatively, the activated AMPA receptors reside outside of the active zone of the otherwise GABA-mediated autapses. This result shows that exogenous expression of BNPI in GABA-containing neurons results in a hybrid phenotype, effectively releasing both the excitatory transmitter glutamate and the inhibitory transmitter GABA from the same neuron.
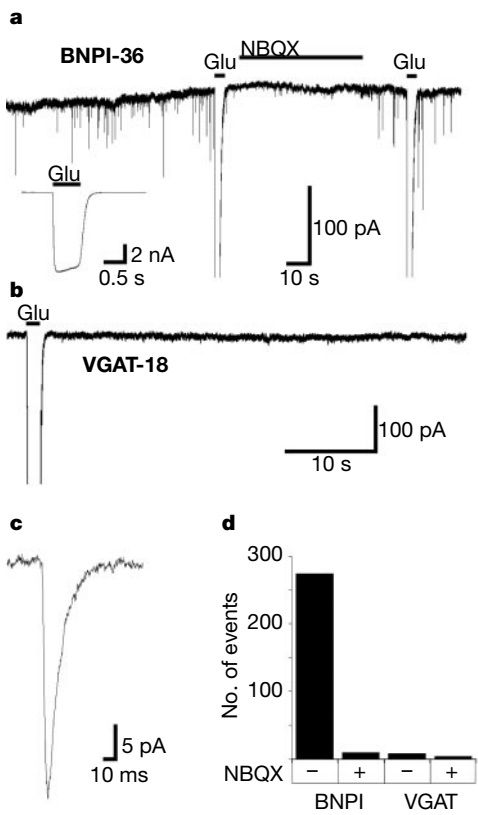

Figure 3 Quantal release of glutamate from BNPI expressing BON cells detected by AMPA-receptor-expressing reporter cells. **a**, HEK293 cells expressing a non-desensitizing AMPA receptor were whole-cell voltage clamped at -70 mV and manipulated into proximity with BON cells expressing BNPI. Acetylcholine was applied at $10-100$ μM to induce secretion from BON cells. The sensitivity of the HEK293 cell to glutamate was intermittently tested by application of exogenous L-glutamate (1 mM, black bars; also see inset). Spike-like inward currents were observed that were stimulated 2.8-fold on acetylcholine application. These events were blocked by NBQX and reversed direction on depolarization to positive potentials (not shown). **b**, An example recording from a HEK/VGAT-18 pair under identical experimental conditions as shown in **a**. Acetylcholine, but not NBQX was added to the external medium. **c**, Average response from 16 events from the same cell as shown in **a**. **d**, Event statistics in absence and presence of NBQX. A total of 1,200 s recording time from 14 experiments on BNPI-36 cells and 900 s from 7 experiments in VGAT-18 cells were analysed.
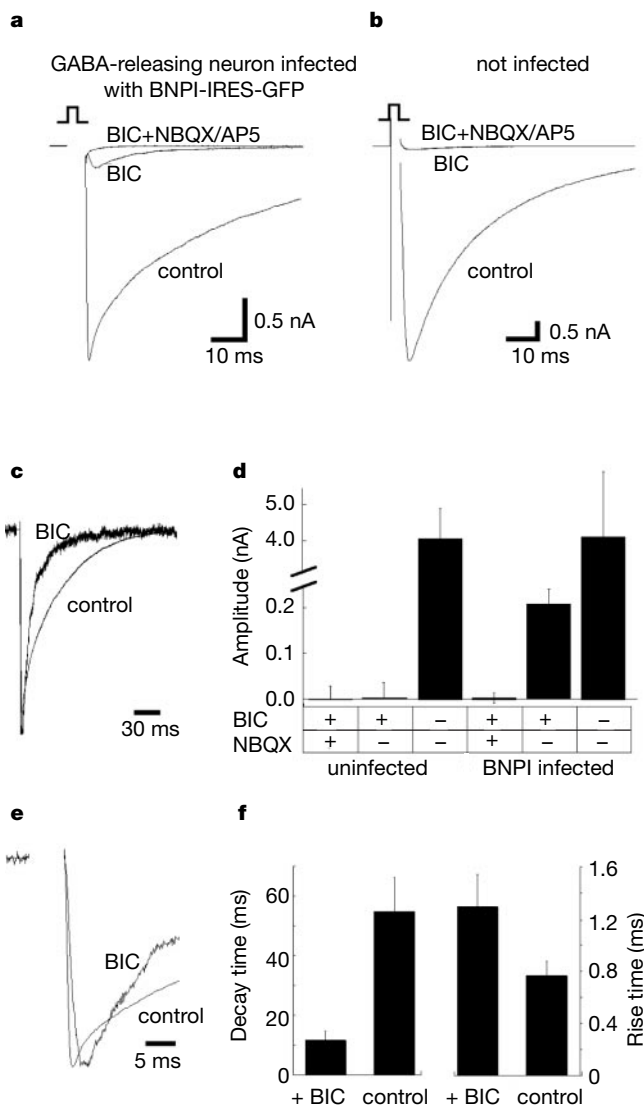

Figure 4 Co-release of GABA and glutamate from BNPI-expressing GABA-containing hippocampal neurons in autaptic culture. **a**, Autaptic response from a hippocampal GABA-containing neuron infected with BNPI-SFV virus. Shown are three superimposed IPSCs, one in absence of blockers showed a typical robust slowly decaying inward current (control). This response was not completely blocked by saturating concentrations of bicuculline (BIC, 30 μM) and picrotoxin (100 μM). The remaining component was blocked by addition of NBQX (30 μM) and AP-5 (50 μM). **b**, Three superimposed IPSCs of an uninfected GABA-containing neuron. The current under control conditions was blocked by bicuculline and picrotoxin (BIC). Addition of NBQX and AP5 has no further effect on the block. **c**, The current transients in BIC+NBQX+AP5 were subtracted from the two other current components taken from **a**, and the inward currents were normalized to illustrate the time course of the two current components. **d**, Statistics of control, BIC and BIC+NBQX amplitudes from BNPI-infected and uninfected GABA-containing neurons. **e**, Expanded time axis of **c**. The evoked NBQX-sensitive current showed a delayed onset. **f**, Statistics of current-decay and current-rise time constants for evoked responses under control and bicuculline conditions. The intracellular solution contained 120 mM Cl$^-$.

Together, the data described above provide conclusive evidence that BNPI functions as vesicular glutamate transporter with properties identical to those observed for glutamate uptake by isolated synaptic vesicles. In fact, our data show that no other component is needed to make a neuron store glutamate in synaptic vesicles and release it by exocytosis upon stimulation. Thus, the vesicular glutamate transporter is the only specific component that is responsible for the transmitter selectivity of glutamate-releasing neurons and thus sets them apart from neurons containing other neurotransmitters. However, the involvement of Na^+-dependent phosphate transport activity observed upon expression of BNPI (refs 1, 2) needs to be clarified. We cannot exclude that glutamate and phosphate transport are somehow linked, for example, that the transporter possesses a mode in which glutamate is exchanged for phosphate (in agreement with the opposite orientation of the two transport activities) with sodium providing some charge compensation.

Is BNPI the only vesicular glutamate transporter? In *C. elegans*, loss-of-function mutation in the BNPI orthologue eat-4 leads to impairment but not to a complete loss of glutamate-mediated neurotransmission[14,15]. Such loss would be expected when the vesicles are not filled with glutamate. However, database searches yielded at least five *C. elegans* homologues of BNPI (accession numbers S40767, Q10046, T23589, Q03567 and S28286), one of which is closely related to eat-4 (S40767), indicating that these additional molecules may operate alongside eat-4 as a vesicular glutamate transporter. Similarly, a human complementary DNA encoding a close relative of BNPI (DNPI, 80% sequence identity with BNPI) has recently been isolated[16]. Thus, it appears that BNPI represents a small family of conserved vesicular glutamate transporters that are, at least in part, functionally redundant. □

Methods

Plasmids and antibodies

The cDNAs corresponding to the open reading frame of rat BNPI and rat VGAT were amplified by polymerase chain reaction using as a template cDNA that was reverse-transcribed from rat brain total RNA, subcloned into pcDNA3.1 (Invitrogen) at *Hin*dIII–*Xho*I and *Bam*HI–*Xba*I sites, respectively, and the sequences were confirmed. The 1.7 kilobases (kb) of *Nhe*I/*Xho*I fragment from BNPI–pcDNA3.1 and the 1.6 kb of *Pme*I fragment from VGAT–pcDNA3.1 were further subcloned into pIRES2–EGFP (Clontech) at *Nhe*I–*Xho*I and *Sma*I site, respectively. For the Semliki-forest virus (SFV) construct for BNPI, 2.9 kb of *Pme*I/*Dra*I fragment from BNPI–pIRES2–EGFP, which contains open reading frame of BNPI and the internal ribosome entry site (IRES) followed by EGFP were cloned into pSFV1 (Gibco BRL) at *Sma*I site. Direction of the insert was confirmed by restriction mapping. The virus was prepared as described[17]. A rabbit polyclonal antibody directed against the amnino-terminal part of rat BNPI was generated by injecting the synthetic peptide (EKRQEGAETLELSAD-C; residues 24–38) which corresponds to the predicted amino-acid sequence of rat BNPI (ref. 1). Other antibodies used in this study are described elsewhere[7].

BON stable transfectants

BON cell line, human pancreatic tumour cells, were cultured in Dulbecco's MEM/Nut mix F-12 (1:1), supplemented with 10% fetal bovine serum, 100 IU ml^{-1} penicillin and 100 μg ml^{-1} streptomycin. BNPI–pIRES2–EGFP, VGAT–pIRES2–EGFP or pIRES2–EGFP without insert was used for transfecting cells (20 μg) by means of the calcium-phosphate method[18]. The transfected cells were then selected in the presence of 800 μg ml^{-1} of G418 and the resulting clones were screened for EGFP fluorescence by fluorescence microscopy. The protein expression of BNPI and VGAT in resulting clones were further confirmed by both immunofluorescence and immunoblotting by using specific antibodies.

Membrane preparation from BON cells and neurotransmitter uptake assay

BON stable clones cultured on 15-cm dishes were washed twice with ice-cold PBS and then collected in 0.32 M sucrose, 4 mM HEPES-NaOH, pH 7.4. The cells were then homogenized using a ball-bearing homogenizer (10 μm clearance). The resulting homogenate was cleared by centrifugation at 10,000g for 5 min to remove the nuclei and cell debris. The supernatant was sedimented by centrifugation at 200,000g for 20 min in TLA120.2 rotor. The resulting membrane pellet was resuspended in 0.32 M sucrose, 4 mM KCl, 4 mM MgSO$_4$, 10 mM HEPES-KOH, pH 7.4 (uptake assay buffer). Neurotransmitter uptake assays were carried out as described previously with slight modifications[7,19]. The reactions were started by incubating 50 μg membrane fraction with 40 μM glutamate or GABA containing 2 μCi [^{3}H]glutamate or [^{3}H]GABA (both from NEM) in the presence of 2 mM

ATP. Proton uncoupler, FCCP (final concentration, 46 μM) and a variety of additives were added when indicated.

Neuronal cell culture and electrophysiology

HEK293 cells were transfected with non-desensitizing AMPA-receptors (GluR1L497Y or the GluR2 homologue GluR2QL504Y; ref. 13) using standard procedures[18]. After 24–72 h after transfection, the GluR-expressing cells were identified either by co-transfecting pDsRed1-N1 (Clontech) or by employing a bicistronic pcDNA3 vector with an additional IRES–DsRed insert. BON cells expressing either BNPI or VGAT and EGFP as a marker were added at a density so that they reached 70% confluency in 24 h when experiments were performed. Spike-like inward currents were not counted if they had rise and decay time constants that were not consistent with receptor kinetics of the non-desensitizing GluR1/2. Hippocampal mouse neurons were cultured on microislands using standard procedures[20] and plated at low density (500 cells cm^{-2}). The neuronal medium was serum-free (neurobasal medium A+B27, Gibco BRL). Experiments from inhibitory neurons were performed at 10–20 days *in vitro* and 24–27 h after addition of the SFV virus. The standard extracellular medium contained (in mM): NaCl, 140; KCl, 2.4; HEPES, 10; glucose, 10; CaCl$_2$, 4; MgCl$_2$, 4. The osmolarity was 300 mOsm and the pH was 7.3.

Solutions were applied using an array of quartz flow pipes positioned within 100–200 μm of the neuron, and connected to gravity-fed reservoirs. Each flow pipe was controlled by solenoid valves and was moved with a piezoelectric device under the control of computer software[21]. Patch pipette (borosilicate) resistance was 2–3.5 MΩ. Pipette solutions for neurons included (in mM): KCl, 120; HEPES, 10; EGTA, 1; MgCl$_2$, 4.6; Na$_4$ATP, 4; Creatinephosphate, 15; creatinephosphokinase 50 U ml^{-1}. Pipette solutions for HEK cells included (in mM) CsF, 140; HEPES, 10; EGTA, 10; NaCl, 10. The pH was 7.3 and the osmolarity was 300 mOsm. Currents were recorded using an Axopatch 200A or 200B amplifier (Axon). Series resistance was 60–90% compensated as was cell capacitance (5–25 pF). Electrophysiological data were acquired on an IBM 586 clone (Pclamp 7-8, Axon) and analysed on a Macintosh (AXOGRAPH4, Axon). The acquisition rate was 2–10 kHz, and data were filtered at 1–2 kHz. Data are expressed as means ± s.e.m.

Others

Purification of synaptic vesicles from rat brain, immuno-isolation and immunoblot analyses were performed as described[7,22]. For peptide microsequencing, protein spots, neighbouring that of synaptotagmin, from several Commassie-stained gels were pooled, concentrated by Funnel-Well SDS–polyacrylamide gel electrophoresis[23] and digested with trypsin *in situ*. The resulting tryptic fragments eluted from the gel matrix were purified using reverse-phase high-performance liquid chromatography and subjected to laser desorption mass spectrometry before microsequencing[5].

1. Ni, B., Rosteck, P. R. Jr., Nadi, N. S. & Paul, S. M. Cloning and expression of a cDNA encoding a brain-specific Na(+)-dependent inorganic phosphate cotransporter. *Proc. Natl Acad. Sci. USA* **91**, 5607–5611 (1994).
2. Ni, B. *et al.* Molecular cloning, expression, and chromosomal localization of a human brain-specific Na$^+$-dependent inorganic phosphate cotransporter. *J. Neurochem.* **66**, 2227–2238 (1996).
3. Bellocchio, E. E. *et al.* The localization of the brain-specific inorganic phosphate transporter suggests a specific presynaptic role in glutamatergic transmission. *J. Neurosci.* **18**, 8648–8659 (1998).
4. Reimer, R. J., Fon, E. A. & Edwards, R. H. Vesicular neurotransmitter transport and the presynaptic regulation of quantal size. *Curr. Opin. Neurobiol.* **8**, 405–412 (1998).
5. Hartinger, J., Stenius, K., Hogemann, D. & Jahn, R. 16-BAC/SDS-PAGE: a two-dimensional gel electrophoresis system suitable for the separation of integral membrane proteins. *Anal. Biochem.* **240**, 126–133 (1996).
6. Dent, J. A., Davis, M. W. & Avery, L. avr-15 encodes a chloride channel subunit that mediates inhibitory glutamatergic neurotransmission and ivermectin sensitivity in Caenorhabditis elegans. *EMBO J.* **16**, 5867–5879 (1997).
7. Takamori, S., Riedel, D. & Jahn, R. Immunoisolation of GABA-specific synaptic vesicles defines a functionally distinct subset of synaptic vesicles. *J. Neurosci.* **20**, 4904–4911 (2000).
8. Parekh, D. *et al.* Characterization of a human pancreatic carcinoid *in vitro*: morphology, amine and peptide storage, and secretion. *Pancreas* **9**, 83–90 (1994).
9. Naito, S. & Ueda, T. Adenosine triphosphate-dependent uptake of glutamate into protein I-associated synaptic vesicles. *J. Biol. Chem.* **258**, 696–699 (1983).
10. Maycox, P. R., Hell, J. W. & Jahn, R. Amino acid neurotransmission: spotlight on synaptic vesicles. *Trends Neurosci.* **13**, 83–87 (1990).
11. Maycox, P. R., Deckwerth, T., Hell, J. W. & Jahn, R. Glutamate uptake by brain synaptic vesicles. Energy dependence of transport and functional reconstitution in proteoliposomes. *J. Biol. Chem.* **263**, 15423–15428 (1988).
12. Hell, J. W., Maycox, P. R. & Jahn, R. Energy dependence and functional reconstitution of the gamma-aminobutyric acid carrier from synaptic vesicles. *J. Biol. Chem.* **265**, 2111–2117 (1990).
13. Stern-Bach, Y., Russo, S., Neuman, M. & Rosenmund, C. A point mutation in the glutamate binding site blocks desensitization of AMPA receptors. *Neuron* **21**, 907–918 (1998).
14. Raizen, D. M. & Avery, L. Electrical activity and behavior in the pharynx of Caenorhabditis elegans. *Neuron* **12**, 483–495 (1994).
15. Lee, R. Y., Sawin, E. R., Chalfie, M., Horvitz, H. R. & Avery, L. EAT-4, a homolog of a mammalian sodium-dependent inorganic phosphate cotransporter, is necessary for glutamatergic neurotransmission in Caenorhabditis elegans. *J. Neurosci.* **19**, 159–167 (1999).
16. Aihara, Y. *et al.* Molecular cloning of a novel brain-type Na(+)-dependent inorganic phosphate cotransporter. *J. Neurochem.* **74**, 2622–2625 (2000).
17. Ashery, U., Betz, A., Xu, T., Brose, N. & Rettig, J. An efficient method for infection of adrenal chromaffin cells using the Semliki Forest virus gene expression system. *Eur. J. Cell Biol.* **78**, 525–532 (1999).
18. Chen, C. & Okayama, H. High-efficiency transformation of mammalian cells by plasmid DNA. *Mol. Cell. Biol.* **7**, 2745–2752 (1987).

19. Hell, J. W., Maycox, P. R., Stadler, H. & Jahn, R. Uptake of GABA by rat brain synaptic vesicles isolated by a new procedure. *EMBO J.* **7,** 3023–3029 (1988).
20. Bekkers, J. M. & Stevens, C. F. Excitatory and inhibitory autaptic currents in isolated hippocampal neurons maintained in cell culture. *Proc. Natl Acad. Sci. USA* **88,** 7834–7838 (1991).
21. Rosenmund, C., Feltz, A. & Westbrook, G. L. Synaptic NMDA receptor channels have a low open probability. *J. Neurosci.* **15,** 2788–2795 (1995).
22. Hell, J. W. & Jahn, R. in *Cell Biology: a Laboratory Handbook* 1st edn (ed. Celis, J. E.) 567–574 (Academic, New York, 1994).
23. Lombard-Platet, G. & Jalinot, P. Funnel-well SDS-PAGE: a rapid technique for obtaining sufficient quantities of low-abundance proteins for internal sequence analysis. *Biotechniques* **15,** 668–670, 672 (1993).

Topological restriction of SNARE-dependent membrane fusion

Francesco Parlati, James A. McNew*, Ryouichi Fukuda*, Rebecca Miller, Thomas H. Söllner & James E. Rothman

Cellular Biochemistry and Biophysics Program, Memorial Sloan Kettering Cancer Center, 1275 York Avenue, Box251 New York, New York 10021, USA

To fuse transport vesicles with target membranes, proteins of the SNARE (soluble *N*-ethylmaleimide-sensitive factor attachment protein receptors) complex must be located on both the vesicle (v-SNARE) and the target membrane (t-SNARE)[1]. In yeast, four integral membrane proteins, Sed5, Bos1, Sec22 and Bet1 (refs 2–6), each probably contribute a single helix to form the SNARE complex that is needed for transport from endoplasmic reticulum to Golgi[7–11]. This generates a four-helix bundle[12], which ultimately mediates the actual fusion event[13]. Here we explore how the anchoring arrangement of the four helices affects their ability to mediate fusion. We reconstituted two populations of phospholipid bilayer vesicles, with the individual SNARE proteins distributed in all possible combinations between them. Of the eight non-redundant permutations of four subunits distributed over two vesicle populations, only one results in membrane fusion. Fusion only occurs when the v-SNARE Bet1 is on one membrane and the syntaxin heavy chain Sed5 and its two light chains, Bos1 and Sec22, are on the other membrane where they form a functional t-SNARE. Thus, each SNARE protein is topologically restricted by design to function either as a v-SNARE or as part of a t-SNARE complex.

Full-length versions of Sed5, Bos1 and Bet1 were produced as glutathione-*S*-transferase (GST) fusion proteins in *Escherichia coli* (Fig. 1, lanes 1, 3 and 4). The full-length form of Sec22 was produced in *E. coli* and purified by nickel chromatography by an amino-terminal His_6 tag (Fig. 1, lane 2). To test whether these recombinant proteins, like their native counterparts, have an intrinsic ability to bind one another, we mixed purified Sec22, Bos1 and Bet1 with a bacterial cell lysate containing GST–Sed5, and isolated protein

complexes with glutathione–agarose beads. Almost stoichiometric amounts of Bos1, Sec22 and Bet1 were bound to GST–Sed5 (Fig. 1, lane 5; see legend).

We took an empirical approach, by testing all eight possible (non-redundant) distributions of four distinct SNAREs among two populations (Table 1), to determine which endoplasmic reticulum (ER)-to-Golgi SNARE(s) are required in the same or different vesicle populations to permit membrane fusion. Altogether, there are eight non-redundant combinations in which (1) all four SNAREs are in one vesicle population and none is in the other; (2) any three distinct SNAREs are in one population and the fourth distinct SNARE is in the other; and (3) any two SNAREs are in one population and the remaining two distinct SNAREs are in the other.

We tested all possible combinations of two SNAREs reconstituted in acceptor and two SNAREs in donor vesicles (Fig. 2). Equimolar amounts of SNAREs were mixed in buffer containing octylglucoside before adding lipids and preparing proteoliposomes as described[13]. All possible combinations of these donor and acceptor liposomes (including cases not shown in Table 1 where one SNARE was
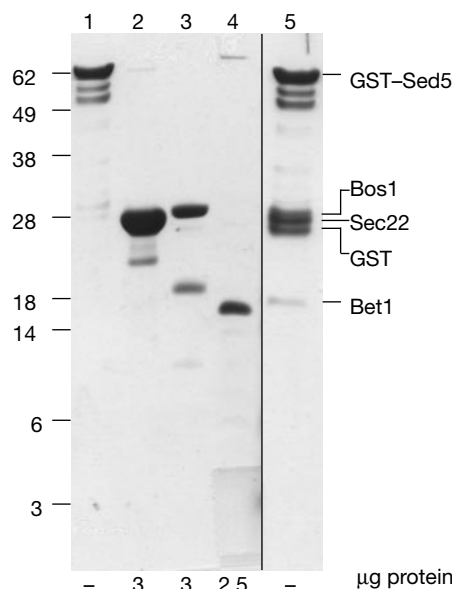

Figure 1 Sed5, Bos1, Sec22 and Bet1 form a quaternary complex. GST–Sed5 lysate was mixed with purified Sec22 (lane 2), Bos1 (lane 3) or Bet1 (lane 4), and 5% of input material was separated. The three SNAREs were isolated in the presence (lane 5) but not in the absence (data not shown) of GST–Sed5. GST–Sed5 isolated in the absence of Sec22, Bos1 and Bet1 is shown for comparison (lane 1). Proteins were analysed by SDS–PAGE and Coomassie blue staining. Note that Bet1 appears at substoichiometric levels because of its poor staining by Coomassie relative to other SNAREs. The stoichiometry of GST–Sed5/Bos1/Sec22/Bet1 in the SNARE complex is 1/1.2/1.2/0.6, as determined by densitometry. Because of the slight differences in the Bet1 migration in lanes 4 and 5 (caused by the presence of non-ionic detergent in lane 4), we confirmed the identity of Bet1 in the SNARE complex isolated in lane 5 by immunoblotting and N-terminal sequencing. Molecular masses in kilodaltons are indicated to the left.

Table 1 Non-redundant combinations of reconstituted SNAREs

Combinations	Acceptor liposomes				Donor liposomes	
4:0	Sed5	Bos1	Sec22	Bet1	–	
3:1	Sed5	Bos1	Sec22		Bet1	
	Sed5		Sec22	Bet1	Bos1	
	Sed5	Bos1		Bet1	Sec22	
		Bos1	Sec22	Bet1	Sed5	
2:2	Sed5	Bos1			Sec22	Bet1
	Sed5		Sec22		Bos1	Bet1
	Sed5			Bet1	Bos1	Sec22

* Present address: Department of Biochemistry and Cell Biology, Rice University, MS140, 6100 Main Street, PO Box 1892, Houston, Texas 77005, USA (J.A.M); Department of Biotechnology, University of Tokyo, 1-1-1 Yayoi, Bunkyo-ku, Tokyo 113-8657, Japan (R.F.).